Optimal Placement of Reconfigurable Intelligent Surfaces with Random Obstacle Distribution

Jingyuan Zhang and Douglas M. Blough
School of Electrical and Computer Engineering
Georgia Institute of Technology, USA
{jingyuan, doug.blough}@ece.gatech.edu

2023 IEEE Wireless Communications and Networking Conference (WCNC) | 978-1-6654-9122-8/23/$31.00 ©2023 IEEE | DOI: 10.1109/WCNC55385.2023.10118608

***Abstract*—Reconfigurable intelligent surfaces (RISs) have been a promising technology to maintain connection performance for millimeter wave (mmWave) communication in non-line-of-sight (NLoS) case by providing an indirect link between access point and user. In this paper, we explore the advantage of multi-RIS deployment to improve connection probability in a scenario with randomly distributed obstacles by solving a modified thinnest covering problem. Optimal RIS deployment in 3D scenario up to six RISs and selection of RIS number based on room size are investigated analytically. A heuristic optimization method of RIS size and orientation is also proposed to guarantee adequate received signal strength. The proposed deployment strategy is validated by simulation that connection probability is significantly improved with only very few RISs.**

***Index Terms*—millimeter wave, multi-RIS deployment, stochastic geometry, connection probability**

I. Introduction

The reconfigurable intelligent surface (RIS) is an emerging technology that can provide a link between transmitter and receiver when the line-of-sight (LoS) path between them is blocked [1]. RIS deployment is a promising approach to improve network coverage in the presence of obstacles, especially for millimeter-wave (mmWave) signals that experience high penetration loss [2]. In view of its promising features, extensive research has been conducted on improving performance of RIS-aided networks in various scenarios by optimizing beamforming for RISs and transmitters, especially given fixed RIS locations [3] [4].

To optimize network-level metrics, RIS placement is an important problem since RIS locations have a significant impact on overall performance. Unfortunately, this is a complicated non-convex optimization problem with a complexity that sharply increases with the number of RISs. The majority of existing works focus on single-RIS placement optimization to fulfill various objectives [5] [6] and only a few consider multi-RIS placement. In [7], throughput improvement of a multi-user cell is considered by placing multiple RISs using a ring-based scheme, while in [8] locations and orientations of multiple RISs are optimized in a 2D scenario with fixed obstacles. To our knowledge, there is no research on optimizing RIS placement in 3D scenarios with randomly distributed obstacles, which is the problem considered herein.

In this paper, we propose a multi-RIS placement strategy to maximize the minimum *connection probability* in an indoor scenario with randomly distributed obstacles. Connection probability is defined as the probability that an unblocked link exists between the access point (AP) and a user, where an unblocked link is either an unobstructed LoS path between the two or an unobstructed LoS path between the user and an RIS together with an unobstructed LoS path between the RIS and the AP. Connection probability is optimized in this paper, because in small to medium sized rooms, any connection will result in a high data rate link in the mmWave band, while no connection obviously means no communication is possible.

The main contributions of this paper are:

- RIS placement in 3D scenario is derived to maximize minimum connection probability given room dimension and the number of RISs, and
- the number of RISs needed to improve connection probability is investigated; i.e. the relationship between RIS number and room dimension is derived analytically or numerically in different scenarios.

II. System model

In this section, the RIS model and stochastic obstacle distribution used in the paper are introduced.

A. RIS pathloss model

When the LoS link between AP and user is blocked, an indirect link where RIS reflects the signal from the AP to a user can be used to maintain connection, as illustrated in Fig. 1(a). Let P_t, λ, G_a, G_u, N, and $G_{ris}(\theta)$ denote the transmit power, wavelength of carrier frequency, antenna gain of the AP, antenna gain of users, the number of elements in an RIS array, and normalized radiation pattern of an RIS element at direction θ, respectively. Herein, the normalized radiation pattern is chosen as $G_{ris}(\theta) = \cos(\theta), \theta \in (-\frac{\pi}{2}, \frac{\pi}{2})$, which is widely used in reflectarrays [9]. For an indirect link where an RIS reflects signal from the AP to a user, the power received by the user is given by

$$P_r = \frac{P_t G_a G_u G_{ris}(\theta_u) G_{ris}(\theta_a) N^2 A^2}{16\pi^2 r_{ra}^2 r_{ru}^2}, \tag{1}$$

where A is effective aperture of one RIS element, r_{ra} and r_{ru} are the distance between an RIS and the AP, and between an RIS and a user, respectively [10]. Herein, A is chosen as the area of one RIS element which is $\frac{\lambda}{2} \times \frac{\lambda}{2}$. The number of RIS elements N and the RIS orientation can be adjusted to achieve adequate signal strength in a targeted area.

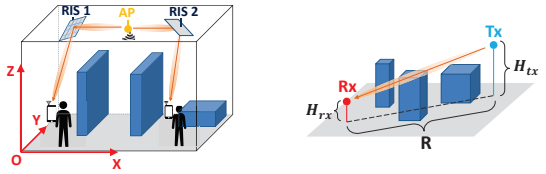

(a) Indirect links assisted by RIS (b) Stochastic geometry model

Fig. 1. Illustration of system model

B. Stochastic obstacle model

We follow numerous prior works on stochastic geometry, e.g. [11], and model obstacles as random cuboids whose centers are located within a targeted area according to a homogeneous Poisson point process (PPP) with density λ_o. Assume that length L and width W of obstacles are uniformly distributed random variables with expectations of $E(L)$ and $E(W)$, respectively, and the angle between an obstacle and the x-axis is a random variable uniformly distributed between 0 and 2π. Besides, let $f_{H_o}(h)$ be the probability density function of obstacle height H_o. Let H_{tx} and H_{rx} denote the height of the transmitter and receiver, respectively. Then, according to [11], the connection probability of a path with horizontal length R between a transmitter and receiver in 3D scenario as shown in Fig. 1(b) is:

$$P_{los}(R) = e^{-\alpha(\beta R+p)}, \tag{2}$$

where $\beta = \frac{2\lambda_o(E(L)+E(W))}{\pi}$, $p = \lambda_o E(L)E(W)$, and α is a scaling factor determined by the distribution of obstacle height as follows:

$$\alpha = 1 - \int_0^1 \int_0^{sH_{tx}+(1-s)H_{rx}} f_{H_o}(h)\,\mathrm{d}h\,\mathrm{d}s. \tag{3}$$

Assume that H_o is a uniformly-distributed random variable over interval $[a_o, b_o]$, and the transmitter height is larger than the receiver height, i.e. $H_{tx} \geq H_{rx}$. Then, the scaling factor α of the link between transmitter and receiver can be calculated as:

$$\alpha = \begin{cases} 1, \text{if } H_{rx} \leq H_{tx} \leq a_o, \\ 1 - \frac{(H_{tx}-a_o)^2}{2(b_o-a_o)(H_{tx}-H_{rx})}, \text{if } H_{rx} \leq a_o \leq H_{tx} \leq b_o, \\ \frac{(H_{rx}-b_o)^2}{2(b_o-a_o)(H_{tx}-H_{rx})} - \frac{(H_{rx}-a_o)^2}{2(b_o-a_o)(H_{tx}-H_{rx})}, \\ \qquad \text{if } H_{rx} \leq a_o \leq b_o \leq H_{tx}, \\ 1 - \frac{(H_{tx}+H_{rx})/2-a_o}{b_o-a_o}, \text{if } a_o \leq H_{rx} \leq H_{tx} \leq b_o, \\ \frac{(b_o-H_{rx})^2}{2(b_o-a_o)(H_{tx}-H_{rx})}, \text{if } a_o \leq H_{rx} \leq b_o \leq H_{tx}. \end{cases} \tag{4}$$

III. Problem Formulation

A. Basic Assumptions

In subsequent analyses, a 3D scenario of a rectangular room with width k and length ak ($a \geq 1$) is considered. Let h_a, h_r, h_u be the height of the AP, RISs and users, respectively. It is assumed that a fixed AP is located in the center of the room near the ceiling with location $\boldsymbol{p}_{ap} = (\frac{k}{2}, \frac{ak}{2}, h_a)$, and RISs are placed around the AP to improve connection probability in the room. Obstacles are modeled based on stochastic geometry introduced in Sec.II-B.

B. Problem Statement

In a room with specific dimensions, it is assumed that a user is randomly located and will connect to the AP by either a LoS link between itself and the AP, or an indirect link through reflection from an RIS to the AP. Then the *connection probability* of a user assisted by RISs is defined as the probability that there exists an unblocked link to the AP, either via the direct LoS path or via an indirect link. Considering randomness of user locations, our objective is to maximize the minimum connection probability over all possible user locations in a target room by placing N_{ris} RISs. The problem can be formulated as follows:

$$\boldsymbol{Q}_{N_{ris}} = \arg\max_{\boldsymbol{Q}_{N_{ris}}} \min_{\boldsymbol{p}_u \in \boldsymbol{P}} P(\boldsymbol{p}_u, \boldsymbol{Q}_{N_{ris}}), \tag{5}$$

where $\boldsymbol{Q}_{N_{ris}}$ is the set of all RIS locations, $\boldsymbol{p}_u \in \mathbb{R}^{1\times 3}$ is the 3D location of the user, $\boldsymbol{P}$ is all possible user locations in a room, and $P(\boldsymbol{p}_u, \boldsymbol{Q}_{N_{ris}})$ is the connection probability for a given user location $\boldsymbol{p}_u$ when the set of RIS locations is $\boldsymbol{Q}_{N_{ris}}$.

The challenge of the above problem includes two aspects. First, there is no closed-form expression of connection probability, especially in a scenario with densely distributed obstacles. According to [12], the connection probabilities of different possible links for one location are approximately independent of each other in scenarios with sparse obstacles, but the independence assumption does not hold for a dense obstacle distribution. Second, it is still intractable to derive closed-form optimal RIS locations, even if we utilize the above independence assumption to simplify the connection probability as follows:

$$\begin{aligned} P(\boldsymbol{p}_u, \boldsymbol{Q}_{N_{ris}}) = 1 - (1 - e^{-\alpha_{ap}(\beta r_{ap}+p)}) \\ \times \prod_{i=1}^{N_{ris}} (1 - e^{-\alpha_i(\beta r_i+p)}) \end{aligned} \tag{6}$$

where r_{ap} is the horizontal distance between the user and the AP, r_i is the horizontal distance between the user and the ith RIS, α_i and α_{ap} are the scaling factors defined by Eq. (3). The complexity of the above problem rises sharply as N_{ris} increases.

IV. Derivation of Optimal RIS Placements

In this section, optimized RIS locations to improve connection probability are given by interpreting the intractable RIS placement problem as a modified thinnest covering problem. Selection of RIS orientation and number of RIS elements is also demonstrated to guarantee proper signal strength in a target area.

Let $\boldsymbol{q}_i \in \mathbb{R}^{1\times 2}$ denote the location of the ith RIS in X-Y plane, $\boldsymbol{Q}_n = \{\boldsymbol{q}_1, \boldsymbol{q}_2, ..., \boldsymbol{q}_n\}$ represent the set of all RIS locations when n RISs are deployed.

A. Modified thinnest covering problem

To make the problem tractable, we adopt the following assumptions to simplify the problem in Eq. (5). First, the AP and all RISs are placed on or near the ceiling so that they are higher than all obstacles. The reason for this is that, given a fixed horizontal distance between RIS and user, the LoS probability increases as the height difference between an RIS and a user increases according to Eq. (2). In addition, the LoS probability of the paths between the AP and each RIS is 1 if they are above all obstacles, which increases the connection probability of indirect links. Second, the user will choose the nearest device, either the AP or the closest RIS, for transmission. In other words, the user will choose a link with highest connection probability based on the first simplification, since such links play a dominant role in the overall connection probability. In this case, the original optimization problem turns into a tractable one as follows:

$$\begin{aligned}\boldsymbol{Q}_{N_{ris}} &= \arg\max_{\boldsymbol{Q}_{N_{ris}}} \min_{\boldsymbol{p}_u \in \boldsymbol{P}} \max_{k \in \{ap,1,2,..,N_{ris}\}} P_k(\boldsymbol{p}_u) \\ &= \arg\max_{\boldsymbol{Q}_{N_{ris}}} \min_{\boldsymbol{p}_u \in \boldsymbol{P}_0} \max_{k \in \{ap,1,2,..,N_{ris}\}} e^{-C(\frac{\beta R_{u,k}}{H_{tx,k}} + \frac{p}{H_{tx,k}})} \\ &= \arg\min_{\boldsymbol{Q}_{N_{ris}}} \max_{\boldsymbol{p}_u \in \boldsymbol{P}_0} \min_{k \in \{ap,1,2,..,N_{ris}\}} (\frac{\beta R_{u,k}}{H_{tx,k}} + \frac{p}{H_{tx,k}}) \end{aligned} \quad (7)$$

where $C = \frac{b_o^2 - a_o^2}{2(b_o - a_o)}$, $\boldsymbol{P}_0$ is the set of all possible user locations with height 0m, $P_k(\boldsymbol{p}_u)$ denotes the connection probability of the link between a user and the AP or a user and the kth RIS, $R_{u,k}$ denotes the horizontal distance between a user and the AP or the kth RIS, and $H_{tx,k}$ is the height of the AP or the kth RIS.

This problem remains difficult to solve when there are multiple RISs for general room configurations. Fortunately, it can be turned into a modified thinnest covering problem if the room is rectangular [13] [14]. The aim of the classical thinnest covering problem is to find locations $\boldsymbol{Q}_N$ of N equal-sized circles with minimum radius to cover a given rectangular, which can be defined as:

$$\boldsymbol{Q}_N = \arg\min_{\boldsymbol{Q}_N} \max_{\boldsymbol{p}_n \in \boldsymbol{P}'} \min_{k \in \{1,2,..,N\}} r_{k,n}, \quad (8)$$

where $r_{k,n}$ is the distance between the center of the kth circle and point $\boldsymbol{p}_n$ which is located in a given rectangle represented as $\boldsymbol{P}'$.

Compared with problem (8), problem (7) can be solved by a modified thinnest covering problem, which is to place two types of circles, one AP circle fixed in the center of the room and N_{ris} RIS circles, so that all circles together cover the targeted rectangular room. Note that all of these circles should have the same $\frac{\beta r}{h} + \frac{p}{h}$, where r is the radius of the circle and h is the height of the corresponding AP or RIS. Since, by assumption, the AP and the RISs are all placed on the ceiling, i.e. at the same height, the problem is simplified to placement of $(1 + N_{ris})$ equal-sized circles with one circle in the center.

B. Multi-RIS deployment

In this section, we solve this modified thinnest covering problem for different numbers of RISs and with different rectangular room dimensions to provide optimal RIS deployments for the considered room configurations. Let r_n denote the radius of AP and RIS circles when n RISs are present.

1) Two RISs: Given two RISs to cover the four corners (see Fig. 2), there are three combinations: (1) one RIS covers A and B and the other RIS covers C and D; (2) one covers A and D and the other covers B and C; (3) one covers A and C and the other covers B and D. For choice (3), the radius of RIS circle is at least $\frac{\|AC\|}{2}$, hence providing no radius reduction compared with the case without RIS. Therefore, choice (3) will not be taken into consideration. For choice (1) and (2), the best RIS locations providing smallest circles are $\{(\frac{ak}{6}, \frac{k}{2}), (\frac{5ak}{6}, \frac{k}{2})\}$ and $\{(\frac{ak}{2}, \frac{3k}{4}), (\frac{ak}{2}, \frac{k}{4})\}$, respectively. Since it is assumed that $a \geq 1$, RIS locations in choice (1) provides smaller RIS circles. Therefore, the optimal RIS locations for 2-RIS case is $\boldsymbol{Q}_2 = \{(\frac{ak}{6}, \frac{k}{2}), (\frac{5ak}{6}, \frac{k}{2})\}$. And the radius of AP and RIS circle is $r_2 = \sqrt{\frac{k^2}{4} + \frac{a^2 k^2}{36}}$.

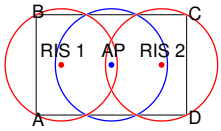

Fig. 2. Optimal locations of 2 RISs

2) 3 RISs: For three RISs, there are three type of layouts: (1) one RIS circle covers A and B and each of the other two RISs covers either of C and D; (2) one RIS circle covers A and D and each of the other two RISs covers either of B and C; (3) one RIS circle covers A and B, one covers C and D, and the last one doesn't cover any corner. Since choice (1) is better than choice (2) due to $a \geq 1$ and choice (3) can not outperform 2-RIS case in Fig. 2, choice (1) is the only feasible deployment. As shown in Fig. 3, there are two possible layouts for choice (1), with difference in that only RIS circles are adequate to cover the entire room if using layout 3RIS-1 illustrated by Fig. 3(a). Since layout 3RIS-2 illustrated by Fig. 3(b) cannot outperform 2-RIS case in Fig. 2, layout 3RIS-1 is the only possible RIS deployment with optimal RIS locations as follows [13]

$$\boldsymbol{Q}_3 = \{(x_3, \frac{k}{2}), (x_3 + \frac{ak}{2}, \frac{3}{4}k), (x_3 + \frac{ak}{2}, \frac{1}{4}k)\}, \quad (9)$$

where $x_3 = \frac{4ka^2 - 3k}{16a}$. The radius of AP and RIS circle is $r_3 = k\frac{\sqrt{16a^4 + 40a^2 + 9}}{16a}$ [13].

To keep minimum radius, the optimal RIS locations when there are three available RISs at most is as follows

$$\boldsymbol{Q}^* = \begin{cases} \boldsymbol{Q}_3, \text{if } 1 \leq a < 1.5, \\ \boldsymbol{Q}_2, \text{if } a > 1.5. \end{cases} \quad (10)$$

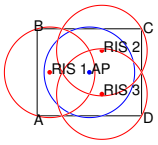

(a) Layout 3RIS-1

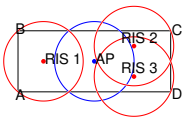

(b) Layout 3RIS-2

Fig. 3. Possible RIS layouts for 3 RISs

3) 4 RISs: Similar as in 2-RIS and 3-RIS cases, where four RISs are deployed, there are three possible layouts: (1) each of the four RISs covers one corner as in Fig.4(a) and Fig.4(b); (2) one RIS circle covers A and B and one covers C and D as in Fig.4(c) and Fig.4(d); (3) one RIS covers corner A and B and each of any other two RISs covers corner C and D, which can be replaced by layouts of three RISs and will not be taken into consideration.

To keep minimum radius, the optimal RIS locations when there are four RISs at most is as follows

$$\boldsymbol{Q}^{*} = \begin{cases} \boldsymbol{Q}_4^{a,2}, \text{if } 1 \le a < \sqrt{3}, \\ \boldsymbol{Q}_4^{a,1}, \text{if } \sqrt{3} \le a < \frac{5}{2}, \\ \boldsymbol{Q}_4^{b}, \text{if } a \ge \frac{5}{2}, \end{cases} \tag{11}$$

where the optimal RIS locations for layout 4RIS-(a)-1, 4RIS-(a)-2 and 4RIS-(b) are given by

$$\boldsymbol{Q}_4^{a,1} = \{(x_4^{a,1}, \frac{3}{4}k), (x_4^{a,1}, \frac{1}{4}k), (ak - x_4^{a,1}, \frac{1}{4}k), (ak - x_4^{a,1}, \frac{3}{4}k)\}, \tag{12}$$

$$\boldsymbol{Q}_4^{a,2} = \{(\frac{ak}{4}, \frac{3k}{4}), (\frac{ak}{4}, \frac{k}{4}), (\frac{3ak}{4}, \frac{k}{4}), (\frac{3ak}{4}, \frac{3k}{4})\}, \tag{13}$$

$$\boldsymbol{Q}_4^{b} = \{(\frac{ak}{10}, \frac{k}{2}), (\frac{3ak}{10}, \frac{k}{2}), (\frac{7ak}{10}, \frac{k}{2}), (\frac{9ak}{10}, \frac{k}{2})\}, \tag{14}$$

where $x_4^{a,1} = \frac{ak}{3} - \frac{k}{12}\sqrt{(2a-3)(2a+3)}$.

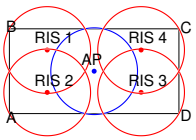

(a) Layout 4RIS-(a)-1

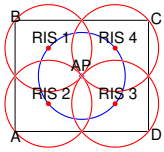

(b) Layout 4RIS-(a)-2

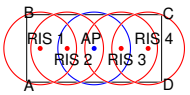

(c) Layout 4RIS-(b)

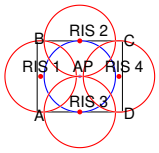

(d) Layout 4RIS-(c)

Fig. 4. Optimal locations of 4 RISs

4) 5 RISs: For five RISs, there are three type of layouts: (1) one RIS circle covers A and B and one covers C and D as in Fig. 5(a); (2) each of four RISs covers one corner as in Fig. 5(b) and Fig. 5(c); (3) one RIS covers corner A and B and each of any other two RISs covers corner C and D, which can be replaced by layouts of three or four RISs and will not be taken into consideration.

For layout (a) in Fig. 5(a), optimal RIS locations and minimum circle size are [13]:

$$\begin{cases} \boldsymbol{Q}_5^{a} = \{(x_5^a, \frac{1}{2}k), (2x_5^a + r_5^a, k), (2x_5^a + r_5^a, 0), \\ \qquad (3x_5^a + 2r_5^a, \frac{1}{2}k), (5x_5^a + 2r_5^a, \frac{1}{2}k)\}, \\ r_5^a = k\frac{3\sqrt{a^2+8}-a}{16}, \end{cases} \tag{15}$$

where $x_5^a = \frac{3ak}{16} - \frac{k}{16}\sqrt{a^2+8}$.

Layout 5RIS-(b)-1 in Fig. 5(b) and layout 5RIS-(b)-2 in Fig. 5(c) are two similar cases which are used for different room dimensions. For layout 5RIS-(b)-1, the optimal RIS locations are represented using RIS circle radius r_5^b as follows:

$$\boldsymbol{Q}_5^{b,1} = \{(x_1, y_1), (x_2, y_2), (x_1, 0), (ak - x_1, y_1), (ak - x_2, y_2)\} \tag{16}$$

where

$$\begin{cases} x_1 = \frac{ak}{4} - \frac{\sqrt{4(r_5^b)^2 - k^2}}{4}, \\ y_1 = k - \sqrt{(r_5^b)^2 - {x_1}^2}, \\ x_2 = \frac{1}{2}\sqrt{4(r_5^b)^2 - (k - 2\sqrt{(r_5^b)^2 - {x_1}^2})^2}, \\ y_2 = \frac{k}{2} - \sqrt{(r_5^b)^2 - {x_1}^2}. \end{cases} \tag{17}$$

In order to get values of optimal locations, we have $\frac{ak}{2} - 2x_2 = r_5^b$. It turns out that r_5^b is a root of Eq. (18). The optimal r_5^b should be the minimal value among real roots larger than $\frac{k}{2}$.

$$\begin{aligned} &(144 - 48a^4)(r_5^b)^4 + k(60a - 16a^3)(r_5^b)^3 + \\ &k^2(4a^4 - \frac{47}{4}a^2 - \frac{27}{2})(r_5^b)^2 - k^3(\frac{9}{4}a^3 + \frac{45}{16}a)r_5^b + \\ &k^4(\frac{9}{16}a^4 + \frac{45}{32}a^2 + \frac{81}{256}) = 0. \end{aligned} \tag{18}$$

Similarly, the optimal RIS locations for layout 5RIS-(b)-2 in Fig.5(c) are

$$\boldsymbol{Q}_5^{b,2} = \{(x_1^*, y_1), (x_2, y_2), (x_1, 0), \tag{19}$$

$$(ak - x_1^*, y_1), (ak - x_2, y_2)\} \tag{20}$$

where $x_1^* = \frac{ak}{2}$, y_1, x_2, y_2 are defined as in Eq. (17) where x_1 is replaced by x_1^*. It turns out that r_5^b is the minimum positive real root of the following fourth order polynomial equation

$$\begin{aligned} &(r_5^b)^4 - 2ka(r_5^b)^3 + k^2(a^2 - 14)(r_5^b)^2 - \\ &2k^3 a r_5^b + k^4(1 + a^2) = 0. \end{aligned} \tag{21}$$

By numerical simulation, a room can support layout 5RIS-(b)-2 if $a \le 1.9832$, while layout 5RIS-(b)-1 if $a > 1.9832$.

To keep minimum radius, the optimal RIS locations when there are five RISs available at most is as follows

$$\boldsymbol{Q}_5^{*} = \begin{cases} \boldsymbol{Q}_5^{b,2}, \text{if } 1 \le a <= 1.9832, \\ \boldsymbol{Q}_5^{b,1}, \text{if } 1.9832 < a <= 2.7946, \\ \boldsymbol{Q}_5^{a}, \text{if } 2.7946 < a < \frac{5}{3}\sqrt{3}, \\ \boldsymbol{Q}_4^{b}, \text{if } a \ge \frac{5}{3}\sqrt{3}. \end{cases} \tag{22}$$

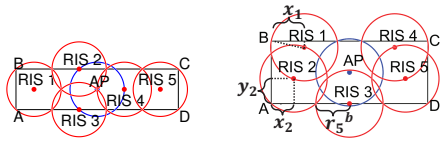

(a) Layout 5RIS-(a)

(b) Layout 5RIS-(b)-1

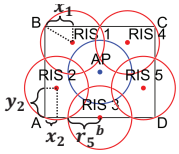

(c) Layout 5RIS-(b)-2

Fig. 5. Optimal locations of 5 RISs

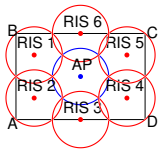

(a) Layout 6RIS-(a)

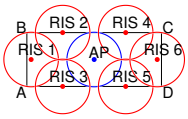

(b) Layout 6RIS-(b)

(c) Layout 6RIS-(c)

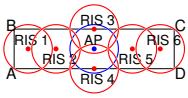

(d) Layout 6RIS-(d)

Fig. 6. Optimal locations of 6 RISs

5) 6 RISs: For six RISs, there are three type of layouts: (1) each of four RISs covers one corner as in Fig. 6(a); (2) one RIS circle covers A and B and one covers C and D as in Fig. 6(b)–6(d); (3) one RIS covers A and B and each of any other two RISs covers C and D, which can be replaced by layouts with fewer RISs and will not be taken into account.

To keep minimum radius, the optimal RIS locations when there are six RISs available at most is as follows

$$\boldsymbol{Q}_{\boldsymbol{6}}^{*}=\begin{cases}\boldsymbol{Q}_{6}^{a}, \text{if } 1 \leq a<\frac{11\sqrt{15}}{15}, \\ \boldsymbol{Q}_{6}^{b}, \text{if } \frac{11\sqrt{15}}{15} \leq a<\frac{7\sqrt{3}}{3}, \\ \boldsymbol{Q}_{6}^{c}, \text{if } a \geq \frac{7\sqrt{3}}{3},\end{cases} \tag{23}$$

where the optimal RIS locations for layout 6RIS-(a), 6RIS-(b), 6RIS-(c) are given by

$$\begin{aligned}\boldsymbol{Q}_{6}^{a}=\{&(x_{6}^{a}, \frac{3k}{4}),(x_{6}^{a}, \frac{k}{4}),(\frac{ak}{2}, 0), \\ &(ak-x_{6}^{a}, \frac{k}{4}),(ak-x_{6}^{a}, \frac{3k}{4}),(\frac{ak}{2}, k)\},\end{aligned} \tag{24}$$

$$\begin{aligned}\boldsymbol{Q}_{6}^{b}=\{&(x_{6}^{b}, \frac{k}{2}),(2x_{6}^{b}+r_{6}^{b}, k),(2x_{6}^{b}+r_{6}^{b}, 0), \\ &(4x_{6}^{b}+3r_{6}^{b}, k),(4x_{6}^{b}+3r_{6}^{b}, 0),(ak-x_{6}^{b}, \frac{k}{2})\},\end{aligned} \tag{25}$$

$$\begin{aligned}\boldsymbol{Q}_{6}^{c}=\{&(\frac{ak}{14}, \frac{k}{2}),(\frac{3ak}{14}, \frac{k}{2}),(\frac{5ak}{14}, \frac{k}{2}), \\ &(\frac{9ak}{14}, \frac{k}{2}),(\frac{11ak}{14}, \frac{k}{2}),(\frac{13ak}{14}, \frac{k}{2})\},\end{aligned} \tag{26}$$

where $x_6^a=\frac{ak}{3}-\frac{k}{6}\sqrt{a^2+\frac{3}{4}}$, and $x_6^b=\frac{3ak}{10}-\frac{k}{5}\sqrt{a^2+5}$.

C. Optimization of RIS size and orientation

In previous sections, RIS locations are optimized to improve connection probability in a targeted room. To ensure that RISs can provide adequate reflected power to cover the entire room, orientation of each RIS is first selected with the aim to maximize the minimum received power in Voronoi regions of this RIS considering a Voronoi digram formed by all RISs and AP, then the number of elements on each RIS is selected to guarantee received power is larger than a predetermined threshold P_{th} in the same region. Let normal vector perpendicular to the ith RIS array represent RIS orientation as $\boldsymbol{n}_i(\theta_i,\phi_i)=[\sin(\theta_i)\cos(\phi_i),\sin(\theta_i)\sin(\phi_i),\cos(\theta_i)]$, where $\theta_i\in[0,\pi]$ and $\phi_i\in[0,2\pi]$. Then the optimal orientation for the ith RIS is given by

$$\{\theta_i,\phi_i\}=\underset{\theta_i\in[0,\pi],\phi_i\in[0,2\pi]}{\arg\max}\ \min_{\boldsymbol{p}_u\in\boldsymbol{P}_{u,i}} P_r(\boldsymbol{n}_i(\theta_i,\phi_i),\boldsymbol{p}_u), \tag{27}$$

where $\boldsymbol{P}_{u,i}$ is set of all points in the Voronoi region of the ith RIS, and $P_r(\boldsymbol{n}_i(\theta_i,\phi_i),\boldsymbol{p}_u)$ is received power at user location $\boldsymbol{p}_u$ given the ith RIS orientation $\boldsymbol{n}_i(\theta_i,\phi_i)$. Given the optimized orientation $\boldsymbol{n}_i$ of the ith RIS, the number of elements on this RIS is determined based on Eq.(1) as follows

$$N_i=\lceil\max_{\boldsymbol{p}_u\in\boldsymbol{P}_{u,i}}\sqrt{\frac{256\pi^2r_{ra}^2r_{ru}^2P_{th}}{P_tG_aG_uG_{ris}(\theta_{\boldsymbol{n}_i}^{\boldsymbol{p}_u})G_{ris}(\theta_{\boldsymbol{n}_i}^{\boldsymbol{p}_{ap}})\lambda^4}}\rceil, \tag{28}$$

where $\theta_{\boldsymbol{n}_i}^{\boldsymbol{p}}$ denotes angle between orientation $\boldsymbol{n}_i$ of the ith RIS and the direction from the ith RIS to point $\boldsymbol{p}$.

V. Numerical Results

In this section, we quantify the minimum connection probability (MCP) improvement for different room dimensions and obstacle densities when RIS locations, orientations and sizes are optimized with the strategies derived in Sec. IV.

The following parameters are fixed for all results in this section. The operation frequency is 60GHz. The equivalent isotropically radiated power (EIRP) of the AP is 43 dBm, and the minimum received power threshold at a user is $P_{th}=-78$ dBm. The room size parameter $k=10$m, and RISs and the AP are placed on the ceiling with a same height 3.5 m. The height of users is assumed to be below 1m. The obstacle height is uniformly distributed in the range of $[a_o,b_o]=[0,3]$, and $E(L)=2$ m and $E(W)=1$ m.

First, in Fig. 7, we evaluate MCP vs. room length for two different obstacle densities. Generally, the results show that RIS benefits are larger when obstacle density is higher and when the room dimensions are unequal (longer room vs. square room). For the higher obstacle density, MCP is improved by about 40% with 6 RISs even when the room is square ($a=1$). When the room dimensions become highly unequal ($a=5$), the MCP is more than 5 times greater with 6 RISs than without RISs. For the lower obstacle density, improvement is relatively modest for the square room, because MCP is already quite high but significant improvement still results for non-square rooms. Comparing different numbers of

RISs, we see that, in general, deploying an odd number of RISs does not improve MCP compared to one fewer RIS. Thus, in general deploying an even number of RISs is preferred. However, in square or nearly square rooms, there is a very modest benefit to odd deployments.

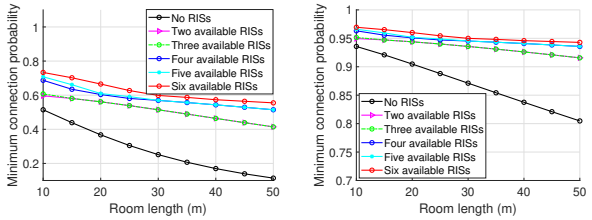

(a) Obstacle density $\lambda_o = 0.1$ (b) Obstacle density $\lambda_o = 0.01$

Fig. 7. Minimum connection probability vs. room length (room width = 10m)

Next, in Fig. 8, we evaluate MCP vs. obstacle density for two different room lengths. The results confirm those from Fig. 7 and extend to extremely high obstacle densities. We still see the most improvement from RIS deployment for higher densities and non-square rooms, and also the preference for an even number of RISs. However, here we also see that, once the obstacle density becomes extremely high, a satisfactory MCP can still not be achieved even with 6 optimized RISs.

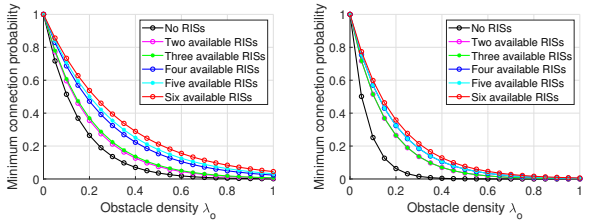

(a) 10m×10m room (b) 10m×30m room

Fig. 8. Minimum connection probability vs. obstacle density

Finally, we investigate the required RIS size to provide adequate signal strength. Here, for each RIS in a given optimal configuration, we first calculate its optimal orientation from Eq. (27) and then we determine the minimum array size to meet the required received power threshold of -78 dBm using Eq. (28). Fig. 9 shows the results. We first note that, for the room sizes shown, none of the array sizes exceed 1,000 elements, which means a typical array size of 32×32 is sufficient to provide the necessary received power. Smaller arrays, such as 16×16 will suffice for rooms up to about 10m×20m with 4 or 6 RISs. As expected, with a smaller number of RISs, larger arrays are needed because each RIS is covering a larger area. This leads to a general conclusion that a larger number of RISs is beneficial since that both reduces the necessary array size and improves the connection probability.

VI. Conclusion

In this paper, optimal deployment of multiple RISs with randomly distributed obstacles is investigated. The optimal RIS locations given room dimension and available number of RISs

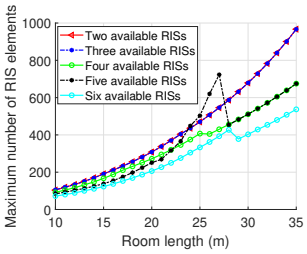

Fig. 9. Maximum number of RIS elements among all RIS arrays vs. room length (room width = 10m)

are derived analytically to improve connection probability between the AP and users. A method to optimize RIS size and orientation is also proposed to guarantee adequate received signal strength. Results show that the proposed RIS deployment strategy significantly improves minimum connection probability compared to not deploying RISs and also demonstrate that deploying an even number of RISs is preferable since odd deployments increase minimum connection probability only marginally.

References

[1] X. Yuan, Y.-J. A. Zhang, Y. Shi, W. Yan, and H. Liu, "Reconfigurable-intelligent-surface empowered wireless communications: Challenges and opportunities," *IEEE Wireless Comm.*, vol. 28, no. 2, pp. 136–143, 2021.

[2] E. Basar, I. Yildirim, and F. Kilinc, "Indoor and outdoor physical channel modeling and efficient positioning for reconfigurable intelligent surfaces in mmWave bands," *IEEE Trans. Comm.*, vol. 69, no. 12, pp. 8600–8611, 2021.

[3] P. Wang, J. Fang, L. Dai, and H. Li, "Joint transceiver and large intelligent surface design for massive MIMO mmWave systems," *IEEE Trans. Wireless Comm.*, vol. 20, no. 2, pp. 1052–1064, 2021.

[4] Y. Xiu, J. Zhao, W. Sun, M. D. Renzo, G. Gui, Z. Zhang, and N. Wei, "Reconfigurable intelligent surfaces aided mmWave NOMA: Joint power allocation, phase shifts, and hybrid beamforming optimization," *IEEE Trans. Wireless Comm.*, vol. 20, no. 12, pp. 8393–8409, 2021.

[5] K. Ntontin, D. Selimis, A.-A. A. Boulogeorgos, A. Alexandridis, A. Tsolis, V. Vlachodimitropoulos, and F. Lazarakis, "Optimal reconfigurable intelligent surface placement in millimeter-wave communications," in *15th European Conf. on Antennas and Propagation*, 2021, pp. 1–5.

[6] H. Lu, Y. Zeng, S. Jin, and R. Zhang, "Aerial intelligent reflecting surface: Joint placement and passive beamforming design with 3D beam flattening," *IEEE Trans. Wireless Comm.*, vol. 20, no. 7, pp. 4128–4143, 2021.

[7] B. Ling, J. Lyu, and L. Fu, "Placement optimization and power control in intelligent reflecting surface aided multiuser system," in *2021 IEEE Global Communications Conference (GLOBECOM)*, 2021, pp. 1–6.

[8] J. Zhang and D. M. Blough, "Optimizing coverage with intelligent surfaces for indoor mmWave networks," in *IEEE INFOCOM 2022 - IEEE Conference on Computer Communications*, 2022, pp. 830–839.

[9] W. L. Stutzman and G. A. Thiele, *Antenna theory and design*. John Wiley & Sons, 2012.

[10] J. Jeong, J. H. Oh, S. Y. Lee, Y. Park, and S.-H. Wi, "An improved path-loss model for reconfigurable-intelligent-surface-aided wireless communications and experimental validation," *IEEE Access*, pp. 1–1, 2022.

[11] T. Bai, R. Vaze, and R. W. Heath, "Analysis of blockage effects on urban cellular networks," *IEEE Trans. Wireless Comm.*, vol. 13, no. 9, pp. 5070–5083, 2014.

[12] M. A. Kishk and M.-S. Alouini, "Exploiting randomly located blockages for large-scale deployment of intelligent surfaces," *IEEE Journal on Selected Areas in Communications*, vol. 39, no. 4, pp. 1043–1056, 2021.

[13] A. Heppes and H. Melissen, "Covering a rectangle with equal circles," *Periodica Mathematica Hungarica*, vol. 34, no. 1, pp. 65–81, 1997.

[14] Y. Liu, Y. Jian, R. Sivakumar, and D. M. Blough, "Maximizing line-of-sight coverage for mmWave wireless LANs with multiple access points," *IEEE/ACM Trans. on Networking*, vol. 30, no. 2, pp. 698–716, 2022.